Supporting Information

Detection and Quantification of Ribosome Inhibition by Aminoglycoside Antibiotics in Living Bacteria Using an Orthogonal Ribosome-Controlled Fluorescent Reporter

Shijie Huang, Xuechen Zhu, and Charles E. Melançon III*

Supporting Information

Table of Contents **Page #**

1. Materials and Methods

1.1. General. All general molecular biological and biochemical reagents, including Luria-Bertani (LB) media (Miller), were purchased from VWR (Atlanta, GA) and were used without further purification. Water used for media was obtained from a Barnstead/Thermolyne HN Ultrapure water purification system. Gentamicin sulfate, paromomycin sulfate, geneticin (G418) sulfate, neomycin sulfate, hygromycin B, amikacin disulfate, sisomicin sulfate, tobramycin sulfate, ribostamycin sulfate, and neamine hydrochloride were purchased from Santa Cruz Biotechnology (Dallas, TX). Kanamycin sulfate was purchased from Genlantis (San Diego, CA). Apramycin sulfate was purchased from Research Products International (Mount Prospect, IL). Restriction enzymes, Phusion DNA polymerase, T4 DNA ligase and calf intestinal alkaline phosphatase were purchased from New England Biolabs (Ipswich, MA). DNA purification and concentration was performed using the DNA Clean & Concentrator Kit; and agarose gel DNA extraction was performed using the Gel DNA Recovery Kit, both from Zymo Research (Irvine, CA). Plasmid extractions were performed using the QIAprep Spin Miniprep Kit from Qiagen (Valencia, CA). Oligonucleotides were obtained from Integrated DNA Technologies (Coralville, IA). DNA sequencing was performed by Genewiz (South Plainfield, NJ). PCR reactions were carried out using a Bio-Rad S1000 thermal cycler. Cell density and fluorescence measurements were taken using a Molecular Devices SpectraMax M2 Multi-Mode Microplate Reader. Plasmid and DNA sequence design and management was conducted using Vector NTI 10 (Life Technologies). Chemically competent *E. coli* cells were prepared using the rubidium chloride method.[1] Standard molecular biological methods, protocols, reagents, and materials[1] were used for PCR, restriction enzyme digestion, ligation, transformation, selection of transformants, agarose gel electrophoresis, gel extraction, and plasmid isolation unless otherwise specified.

1.2. Bacterial strains. E. coli DH5α and *E. coli* TOP10 were used for routine DNA cloning and manipulation. *E. coli* SQ380 (*E. coli* MG1655/Δ*rrn*GADEHBC/prrnC-sacB[2]/ptRNA67[2], S. Quan and C. Squires, unpublished), in which all seven genomic rRNA operons have been deleted and replaced with a single plasmid-borne rRNA operon expressed from the sucrose counterselectable plasmid prrnC-sacB, was used as the starting point for construction of strains capable of detecting ribosome inhibition by aminoglycoside antibiotics.

1.3. Bacterial culture. Routine liquid culture of *E. coli* DH5α and *E. coli* TOP10 for cloning purposes was carried out in 2-5 mL of Luria-Bertani broth in sterile 15 mL conical tubes at 37 °C, 250 rpm overnight (12-16 h). Selection of *E. coli* DH5α and *E. coli* TOP10 transformants was carried out on Luria-Bertani agar plates containing the appropriate antibiotic(s) at 37 °C overnight (12-16 h). All cell growth and fluorescence assays were performed in sterile Cellstar 96-well deep well culture plates sealed with breathable sealing film, with one mL of LB media per well and with appropriate concentrations of the necessary antibiotics (ampicillin - 100 μg/mL, chloramphenicol - 35 μg/mL, kanamycin - 50 μg/mL, spectinomycin – 100 μg/mL), anhydrotetracycline (1-100 ng/mL) and aminoglycoside (1-1024 μM).

1.4. General PCR conditions. Concentrations of template, primers, polymerase, dNTPs, and buffer recommended by NEB for Phusion DNA polymerase were used unless otherwise specified. We employed four types of PCR protocols to construct all fragments and all final constructs not obtained by ligation: Protocol 1) PCR amplification of a single fragment with two primers, Protocol 2) templateless (primer only) assembly with three primers, Protocol 3) two fragment overlap extension PCR, and Protocol 4) COE-PCR (see Section 2.2.1 for an explanation of this method). General PCR programs for each protocol are given below.

Protocol 1		Protocol 2	Protocol 3		Protocol 4	
98 °C	30 s	Same as Protocol 1, but with no template, and with 0.1 µM inside primer, 0.5 µM of each of the two outside primers.	98 °C	30 s	Used 10 nM of each fragment	
98 °C	10 s		98 °C	10 s		
Tm-prim – 5	30 s		Tm-OE – 5	30 s		
72 °C	30 s/kb		72 °C	30 s/kb	98 °C	30 s
Repeat 2 times			Repeat 1-9 times		98 °C	10 s
98 °C	10 s		(primerless)		48-50 °C	30 s
Tm-ext – 5	30 s		Add 0.5 µM of 2 outside		72 °C	15 s/kb
72 °C	30 s/kb		primers		(of final plasmid size)	
Repeat 26 times			98 °C	10 s	Repeat 29-34 times	
72 °C	10 m		Tm-ext – 5	30 s	72 °C	10 m
4 °C	∞		72 °C	30 s/kb	4 °C	∞
			Repeat 29 times			
			72 °C	10 m	Fragment junctions were designed to have Tm of 55 +/- 5 °C	
			4 °C	∞		

Tm-prim = Tm of the portion of the primer that primes to the template
Tm-ext = Tm of the entire primer
Tm-OE = Tm of the junction between fragments

1.5. Enforced replacement by sucrose counterselection. To replace plasmid prrnC-sacB (Kan^R, Suc^S) which is essential in *E. coli* SQ380 because it carries the only cellular copy of the ribosomal RNA (rRNA) operon, with pRRSH2 (Amp^R), pRRSH2-A1408G, or pRRSH2-U1406A, we employed sucrose counterselection against the sacB (sucrose sensitivity gene)-containing plasmid prrnC-sacB. *E. coli* SQ380 competent cells were grown in LB with kanamycin and spectinomycin (essential tRNA-bearing plasmid ptRNA67 has a spectinomycin resistance marker) and transformed with pRRSH2, pRRSH2-A1408G, or pRRSH2-U1406A. Transformants were selected on LB agar with ampicillin and spectinomycin. One colony was picked and grown in LB liquid with ampicillin and spectinomycin overnight, and plated on LB agar with ampicillin, spectinomycin, and 5% (w/v) sucrose. Surviving colonies are resistant to both ampicillin and sucrose, and have therefore gained pRRSH2 and lost prrnC-sacB. Elimination of prrnC-sacB was verified by plasmid isolation and digestion of the resulting plasmid mixture with PvuI, which has 3 recognition sites in prrnC-sacB but only a single site in pRRSH2 and ptRNA67, and therefore gives a distinctive digestion pattern if prrnC-sacB is present. This, rather than replica plate screening of surviving colonies for kanamycin sensitivity, was done because pRRSH2-A1408G and pRRSH2-U1406A confer kanamycin resistance. The resulting strains - SH430 containing pRRSH2, SH386 containing pRRSH2-A1408G, and SH424 containing pRRSH2-U1406A – were used for transformation with plasmids carrying the O-ribosome-based aminoglycoside detection systems (pSH3-KF through pSH14-KF).

1.6. Cell density and fluorescence assays. All cell density and fluorescence measurements were taken in triplicate. 96-well culture plates (1 mL LB per well) with appropriate concentrations of necessary antibiotics and aminoglycoside were inoculated 1:100 from a saturated overnight liquid culture and allowed to grow for 18-24 h at 37 °C, 200 rpm shaking. For cell density assays, 40 µL of sample was taken from each well, diluted 5-fold, and OD_{600} was measured by microplate reader. The OD_{600} of the original culture was calculated by multiplying the reading by the dilution factor (5). For cell pellet fluorescence imaging, cells were pelleted by centrifugation (4,000 *g*, 15 m, 4 °C) and the supernatant was decanted completely. The underside of the plate was illuminated at 365 nm using an ultraviolet handheld lamp and photographed with an 8 megapixel digital camera. For fluorescence quantification, cell pellets were resuspended in 1 mL of ¼× Ringer's solution (30.75 mM NaCl, 1.2 mM, KCl, 1.5 mM $CaCl_2$, pH 7.3-7.4), 200 µL of cells from each well were transferred to black 96-well plates, and GFP fluorescence was measured (excitation = 395 nm, bandwidth = 9 nm; emission = 509 nm, bandwidth = 15 nm). Fluorescence intensities were calculated as fluorescence/OD_{600} of the sample minus fluorescence/OD_{600} of a sample of a non-GFP-expressing *E. coli* strain parental to the strain being analyzed in order to correct for both cell density and *E. coli* auto-fluorescence.

1.7. Calculation of IC_{50}, LD_{50} values and correlation analysis. Aminoglycoside IC_{50} values were calculated by fitting fluorescence data obtained by incubating detection strains SH399 or SH431 with aminoglycosides at concentrations from zero to the concentration that gives maximal fluorescence signal to a sigmoidal equation by non-linear regression. The IC_{50} value is the concentration of aminoglycoside that gives half maximal fluorescence. Aminoglycoside LD_{50} values were calculated by fitting OD_{600} data obtained by incubating the parent aminoglycoside sensitive strain SH434 with aminoglycosides at concentrations from zero to 32 μM (or 1024 μM for neamine and hygromycin B) to a sigmoidal equation by non-linear regression. The LD_{50} value is the concentration of aminoglycoside the gives 50% growth inhibition (an OD_{600} value that is 50% of the maximal OD_{600} value). Correlation between IC_{50} values calculated from fluorescence data and either previously reported IC_{50} values obtained from *in vitro* translation assays (main text reference #28) or LD_{50} values calculated from OD_{600} data were assessed by linear regression analysis. The IC_{50} and LD_{50} values determined, and the results of linear regression are summarized in Figure S6.

2. Vector construction and functional assays

2.1. General notes. All vectors used in this study were designed to avoid any antibiotic resistance markers that encode aminoglycoside modifying enzymes (e.g. kanamycin, apramycin, streptomycin resistance markers) or tetracycline because they would interfere with aminoglycoside detection, or the TetR repressor system, respectively.

2.2. rRNA-expressing plasmids

2.2.1. Construction of pRRSH2. Plasmid pKK3535[3] (11.9 kb), which contains the constitutively expressed *rrnB* ribosomal rRNA operon, pMB1 origin of replication, and ampicillin resistance marker, as well as 4.2 kb of non-essential DNA sequence, was used as the starting point for construction of a simplified, refactored *rrnB*-expressing plasmid pRRSH2 (7.7 kb), which also bears the ampicillin resistance marker, but contains the p15A origin of replication. To construct pRRSH2, we employed concatamerizing overlap extension PCR (COE-PCR, C. Melançon, unpublished), a *de novo* plasmid assembly method developed in our group that is similar to the CPEC method.[4] In COE-PCR, a circular plasmid is obtained by one pot PCR assembly of linear fragments with short (15-25 bp) overlapping ends followed by transformation of competent *E. coli* with the PCR assembly mixture. The 5.8 kb *rrnB* operon was amplified as three fragments from pKK3535 using primer pairs pRRSH-rRNA1-up/pRRSH-rRNA1-dn, pRRSH-rRNA2-up/pRRSH-rRNA2-dn, and pRRSH-rRNA3-up/pRRSH-rRNA3-dn. The fragment containing the promoter and coding region of the ampicillin resistance marker was amplified from pKK3535 using primers pRRSH-AmpR-up and pRRSH-AmpR-dn. The fragment containing the p15A origin of replication was amplified from pRepCM3[5] using primers pRRSH-p15A-up and pRRSH-p15A-dn. The resulting five DNA fragments were assembled by COE-PCR and the reaction mixture was concentrated using the Zymo Clean and Concentrator Kit, and introduced into competent *E.coli* DH5α cells. The final pRRSH2 construct was verified by restriction mapping and sequencing. Primer information is given in the table below. The priming region of each primer is underlined.

primer name	sequence (5' – 3')	amplicon size (bp)	template
pRRSH-rRNA1-up	TTTGGTTGAATGTTGCGCGGTC	2116	pKK3535
pRRSH-rRNA1-dn	CGGTGTCCTGGGCCTCTAGAC		
pRRSH-rRNA2-up	TCTAGAGGCCCAGGACACCGCCCTTTCACGGCGGTAACAG	2022	pKK3535
pRRSH-rRNA2-dn	CTGGTATCTTCGACTGATTTCAGCTCCATCCGCGAGGGACC		
pRRSH-rRNA3-up	GCTGAAATCAGTCGAAGATACCAGCTGGC	1677	pKK3535
pRRSH-rRNA3-dn	AGCTGCTTTCCTGATGCAAAAACG		
pRRSH-AmpR-up	CGTTTTTGCATCAGGAAAGCAGCTGATATCAGACGTCAGGTGGCACTTTTC	1077	pKK3535
pRRSH-AmpR-dn	CATATGATCAATCTAAAGTATATATGAGTAAACTTGGTCTGACAG		
pRRSH-p15A-up	CCAAGTTTACTCATATATACTTTAGATTGATCATATGCTTCGGATCCCTCGAGAGATC	934	pRepCM3
pRRSH-p15A-dn	CCGCGCAACATTCAACCAAAATTACATGTGCGTCAGACCC		

p15A origin of replication fragment sequence. Primer binding sites are underlined, and the p15A origin region is shown in blue.

ATTACATGTGCGTCAGACCCCTTAATAAGATGATCTTCTTGAGATCGTTTTGGTCTGCGCGTAATCTCTTGCTCTGAAAACGAAAAAAC
CGCCTTGCAGGGCGGTTTTTCGAAGGTTCTCTGAGCTACCAACTCTTTGAACCGAGGTAACTGGCTTGGAGGAGCGCAGTCACCAAAAC
TTGTCCTTTCAGTTTAGCCTTAACCGGCGCATGACTTCAAGACTAACTCCTCTAAATCAATTACCAGTGGCTGCTGCCAGTGGTGCTTT
TGCATGTCTTTCCGGGTTGGACTCAAGACGATAGTTACCGGATAAGGCGCAGCGGTCGGACTGAACGGGGGGTTCGTGCATACAGTCCA
GCTTGGAGCGAACTGCCTACCCGGAACTGAGTGTCAGGCGTGGAATTAGACAAACGCGGCCATAACAGCGGAATGACACCGGTAAACCG
AAAGGCAGGAACAGGAGAGCGCACGAGGGAGCCGCCAGGGGGAAACGCCTGGTATCTTTATAGTCCTGTCGGGTTTCGCCACCACTGAT
TTGAGCGTCAGATTTCGTGATGCTTGTCAGGGGGGCGGAGCCTATGGAAAAACGGCTTTGCCGCGGCCCTCTCACTTCCCTGTTAAGTA
TCTTCCTGGCATCTTCCAGGAAATCTCCGCCCCGTTCGTAAGCCATTTCCGCTCGCCGCAGTCGAACGACCGAGCGTAGCGAGTCAGTG
AGCGAGGAAGCGGAATATATCCTGTATCACATATTCTGCTGACGCACCGGTGCAGCCTTTTTTCTCCTGCCACATGAAGCACTTCACTG
ACACCCTCATCAGTGCCAACATAGTAAGCCAGTATACACTCCGCTAGCCCATGGAGATCTCTCGAGGGATCCGAAG

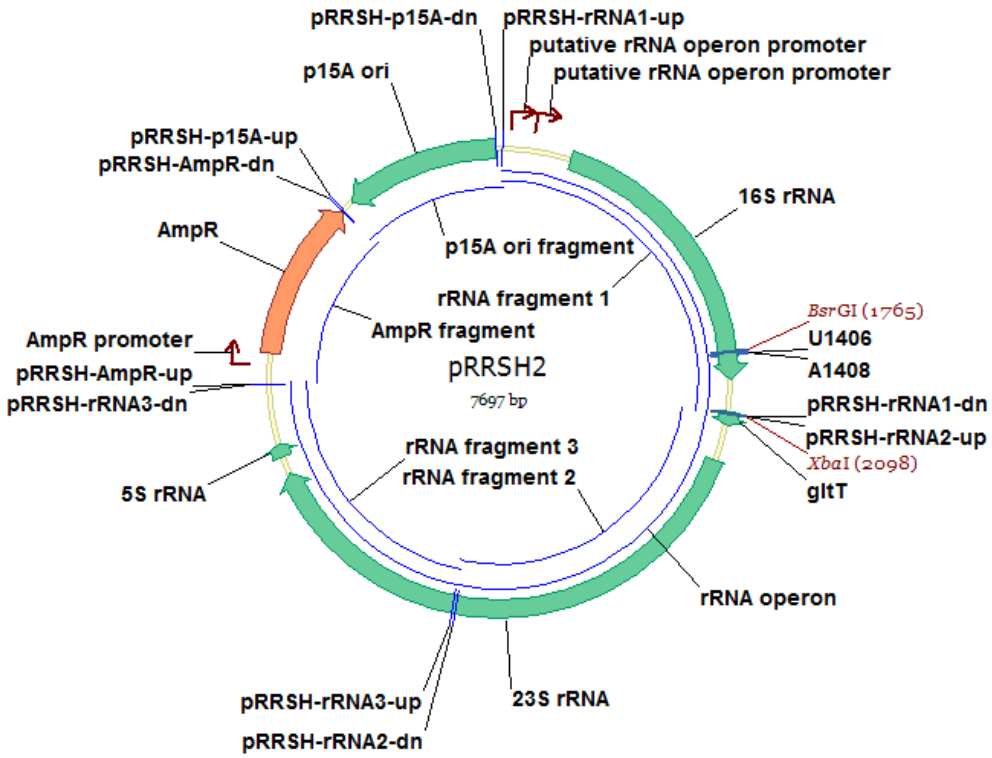

2.2.2. Construction of pRRSH2-A1408G and pRRSH2-U1406A. Both plasmids were constructed from pRRSH2. A 684 bp region of pRRSH2 containing the 16S rRNA A1408 and U1406 sites was amplified in two fragments with the mutation site at the junction of the fragments. In each case, the two fragments were joined by overlap extension PCR, the resulting PCR product digested with BsrGI and XbaI, and cloned into pRRSH2 digested with the same enzymes. For pRRSH2-A1408G, fragment 1 was amplified using primers pRRSH2-A1408G-1 and pRRSH2-A1408G-2, and fragment 2 was amplified using primers pRRSH2-A1408G-3 and pRRSH2-A1408G-4. For pRRSH2-U1406A, fragment 1 was amplified using primers pRRSH2-A1408G-1 and pRRSH2-U1406A-2, and fragment 2 was amplified using primers pRRSH2-U1406A-3 and pRRSH2-A1408G-4. Introduction of the mutation into each plasmid was verified by sequencing the cloned region of the plasmid containing it. The vector map of pRRSH2-A1408G is given as an example. Primer information is given in the table below. The A1408G and U1406A mutation sites are show in bold red in the primers that contain them. The priming region of each primer is underlined.

primer name	sequence (5' – 3')	amplicon size (bp)	template
pRRSH2-A1408G-1	TCTCAAACATCACCCGAAGATGAG	457	pRRSH2
pRRSH2-A1408G-2	CCCGTCGCACCATGGGAGTG		
pRRSH2-A1408G-3	CCATGGTGCGACGGGCGGTGTG	242	pRRSH2
pRRSH2-A1408G-4	GAGGAAGGTGGGGATGACGTC		
pRRSH2-U1406A-2	CCCGACACACCATGGGAGTG (used with pRRSH2-A1408G-1)	457	pRRSH2
pRRSH2-U1406A-3	ACTCCCATGGTGTGTCGGGCGGTG (used with pRRSH2-A1408G-4)	246	

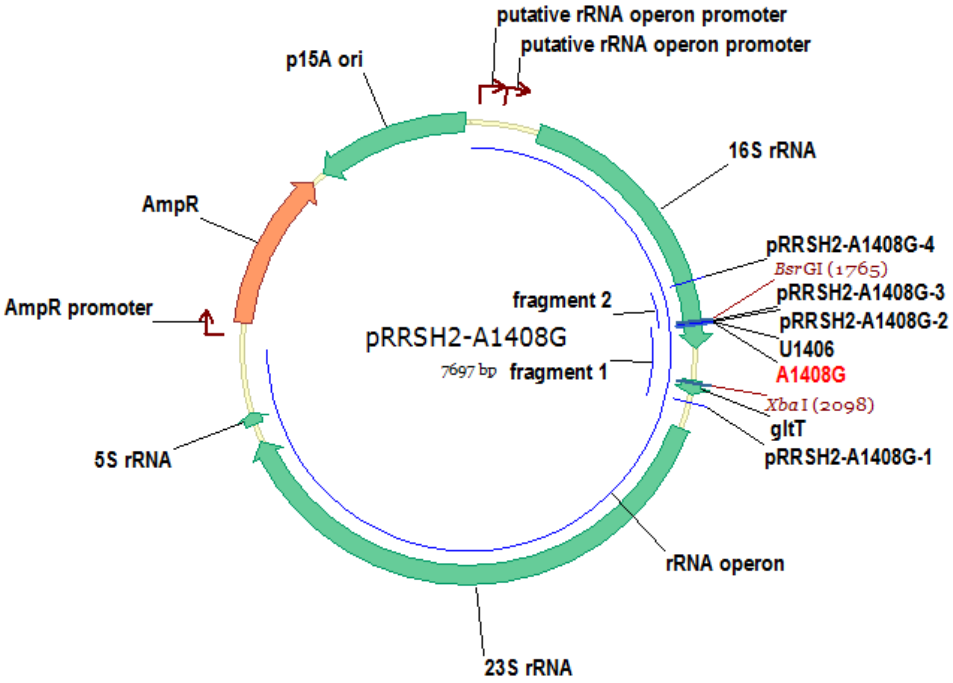

2.2.3. Functional verification of pRRSH2-A1408G and pRRSH2 in E. coli SQ380. The ability of pRRSH2-A1408G to confer aminoglycoside resistance was confirmed through a cell viability assay. *E. coli* SQ380 was transformed with pRRSH2-A1408G; and prrnC-sacB was removed by sucrose counterselection, resulting in *E. coli* SH386. As a control, *E. coli* SQ380 was also transformed with pRRSH2; and prrnC-sacB was removed by sucrose counterselection, resulting in *E. coli* SH430. The growth inhibition of these two strains by various kanamycin concentrations was determined by inoculation of each strain (1:100 dilution of a saturated culture) into ten 1 mL wells of a 96-well culture plate containing LB broth with specific concentrations of kanamycin added (Fig. S1), growth for 24 h at 37°C, 200 rpm shaking, and measurement of the OD_{600}. The results (Fig. S1) clearly demonstrate that *E. coli* SH430, which has no 16S rRNA aminoglycoside resistance mutation, experiences significant growth inhibition at 10 μM kanamycin, and cannot survive at concentrations above 10 μM kanamycin; whereas *E. coli* SH386, which has the A1408G mutation, shows no growth inhibition at any kanamycin concentration tested, indicating that the mutation confers robust resistance to kanamycin at concentrations as high as 500 μM.

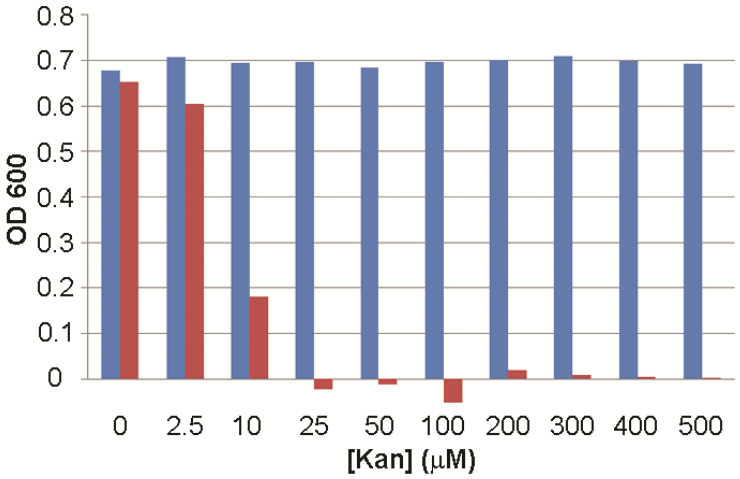

Figure S1. OD_{600} readings of SH386 (A1408G, blue bars) and SH430 (wild-type, red bars) grown in a range of kanamycin concentrations.

2.3 Sequential construction of the reporter plasmid

2.3.1. General notes. The final reporter plasmid, pSH6-KF, was constructed in six steps:

1) construction of pUC19-GFPuv, which contains the *gfp-uv* gene under control of the PLtetO-1 promoter (see section 2.3.2)
2) optimization of the *gfp-uv* 5'-untranslated (5'-UTR) region through construction of a five plasmid series pGBSH1-BCD2, pGBSH1-U2, pGBSH1-26.2, pGBSH1-pET, and pGBSH1-pBEST (see section 2.3.3).
3) replacement of the ampicillin resistance marker with a chloramphenicol resistance marker in pGBSH1-BCD2, the plasmid with the highest *gfp-uv* expression level from Step 2, to give pGBSH3 (see section 2.3.5).
4) insertion of the cassette containing *tetR* with orthogonal Shine-Dalgarno (O-SD) sequence under control of medium strength promoter BBa_J23016 into pGBSH3 to give pGBSH18 (see section 2.3.6).
5) insertion of the cassette containing the orthogonal 16S rRNA (O-16S) under control of the constitutive *lpp* promoter to give reporter plasmid pSH3-KF (see section 2.3.7).
6) optimization of the *tetR* and O-16S promoter strengths for use in *E. coli* SH386 through construction of an eleven plasmid series pSH4-KF through pSH14-KF (see section 2.4.2).

2.3.2. Construction and testing of pUC19-GFPuv. This plasmid, which contains the *gfp-uv* gene under control of the PLtetO-1 promoter/operator[6], pMB1 origin of replication, and ampicillin resistance marker was constructed from four fragments by COE-PCR. The PLtetO-1 promoter/operator was amplified from pSR26_2 (J. Tabor, unpublished) using primers pLTetO1N-up and pLtetO1-dn. The *gfp-uv* gene was amplified from plasmid pET101-GFP[7] using primers pGFP-up and pCL-F2-dn. The pMB1 origin of replication was amplified from pUC19 using primers pCL-F3-pMB1-up and pCL-F3-pMB1-dn. The ampicillin resistance marker was amplified from pUC19 using primers pCL-F4-up and pCL-F4-dn. The resulting four fragments were assembled by COE-PCR. The reaction mixture was concentrated using the Zymo Clean and Concentrator Kit, and introduced into competent *E.coli* DH5α cells. The final construct was verified by restriction mapping and sequencing. Primer information is given in the table below. The priming region of each primer is underlined.

E. coli DH5α transformed with pUC19-GFPuv displayed no fluorescence as determined by plate reader fluorescence assay (see cell density and fluorescence assays section, above, for experimental details). Reasoning that the lack of GFPuv expression was due to a non-optimal chimeric 5'-untranslated region (5'-UTR) derived from fusion of 5'-UTRs from pSR26_2 and pET101-GFP, we next constructed a series of five pUC19-GFPuv derivatives where the 5'-UTR was varied.

primer name	sequence (5' – 3')	amplicon size (bp)	template
pLtetO1N-up	ACAAACTAGTGCGACCCTGCGTATCACGAGGCCCTTTCGTC	159	pSR26_2
pLtetO1-dn	CATGGTGAAGGGCTCCTGAATTCCTTCATTAATGGTCAGTGCGTCCTGCTGATG		
pGFP-up	GAAGGAATTCAGGAGCCCTTCACCATG	1022	pET101-GFP
pCL-F2-dn	CCGGGCCTCTTGCGGGATATC		
pCL-F3-pMB1-up	ATATCCCGCAAGAGGCCCGGGCGGTAATAAGCTTACGGTTATCCACAGAATCAGG	758	pUC19
pCL-F3-pMB1-dn	AGACCCCGTCTAGATAGAAAAGATCAAAGGATCTTCTTGAG		
pCL-F4-up	CTTTGATCTTTTCTATCTAGACGGGGTCTGACGCTCAGTG	1137	pUC19
pCL-F4-dn	GCAGGGTCGCACTAGTTTGTTTATTTTTCTAAATACATTCAAATATGTATCCGCTC		

gfp-uv fragment sequence. Primer binding sites are underlined, the *gfp-uv* coding region is shown in blue with start and stop codons underlined, and the T7 terminator sequence is shown in green.

GAAGGAATTCAGGAGCCCTTCACCATGAGTAAAGGAGAAGAACTTTTCACTGGAGTTGTCCCAATTCTTGTTGAATTAGATGGTGATGT
TAATGGGCACAAATTTTCTGTCAGTGGAGAGGGTGAAGGTGATGCAACATACGGAAAACTTACCCTTAAATTTATTTGCACTACTGGAA
AACTACCTGTTCCATGGCCAACACTTGTCACTACTTTCTCTTATGGTGTTCAATGCTTTTCCCGTTATCCGGATCACATGAAACGGCAT
GACTTTTTCAAGAGTGCCATGCCCGAAGGTTATGTACAGGAACGCACTATATCTTTCAAAGATGACGGGAACTACAAGACGCGTGCTGA
AGTCAAGTTTGAAGGTGATACCCTTGTTAATCGTATCGAGTTAAAAGGTATTGATTTTAAAGAAGATGGAAACATTCTCGGACACAAAC
TCGAATACAACTATAACTCACACAATGTATACATCACGGCAGACAAACAAAAGAATGGAATCAAAGCTAACTTCAAAATTCGCCACAAC
ATTGAAGATGGATCCGTTCAACTAGCAGACCATTATCAACAAAATACTCCAATTGGCGATGGCCCTGTCCTTTTACCAGACAACCATTA
CCTGTCGACACAATCTGCCCTTTCGAAAGATCCCAACGAAAAGCGTGACCACATGGTCCTTCTTGAGTTTGTAACTGCTGCTGGGATTA
CACATGGCATGGATGAGCTCTACAAACTCGAGCACCACCACCACCACCACTGAAAGGGCGAGCTCAATTCGAAGCTTGAAGGTAAGCCT
ATCCCTAACCCTCTCCTCGGTCTCGATTCTACGCGTACCGGTCATCATCACCATCACCATTGAGTTTGATCCGGCTGCTAACAAAGCCC
GAAAGGAAGCTGAGTTGGCTGCTGCCACCGCTGAGCAATAACTAGCATAACCCCTTGGGGCCTCTAAACGGGTCTTGAGGGGTTTTTTG
CTGAAAGGAGGAACTATATCCGGATATCCCGCAAGAGGCCCGG

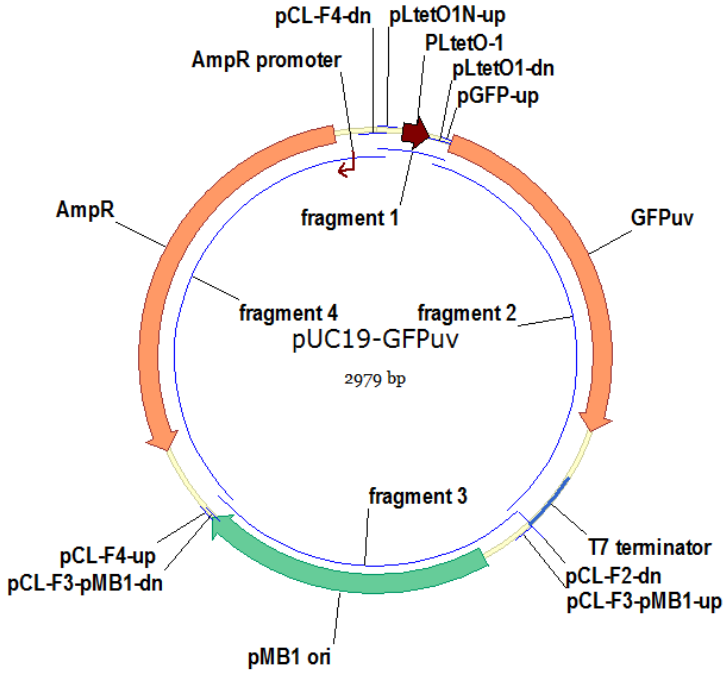

2.3.3. Construction of the pGBSH1 plasmid series. The pGBSH1 plasmid series was constructed by replacement of the *gfp-uv* 5'-UTR on pUC19-GFPuv with 5 different 5'-UTRs. We chose three 5'-UTRs that were reported to be strong [BCD2[8], U2[9], pBEST(unpublished, from Addgene #45784)] and two representing the intact 5'-UTRs associated with the

GFPuv gene in pET101-GFP (pET) and the PLtetO-1 promoter in pSR26_2 (26.2). Additionally, a T0 spacer sequence was added between the ampicillin resistance gene and the PLtetO-1 portion to attempt to minimize any polar effects on GFP expression. The T0 spacer was appended to the 5' end of the PLtetO-1 fragment. Construction of these plasmids was accomplished by five COE-PCR reactions, each employing four fragments, three of which (pMB1 origin, ampicillin resistance marker, T0 spacer-PLtetO-1) were identical in all five reactions, and one (the 5'-UTR-*gfp-uv* fragment) of which was variable. The fragments containing the pMB1 origin and ampicillin resistance marker were identical to those used in construction of pUC19-GFPuv.

The T0 spacer-PLtetO-1 fragment was constructed by three sequential PCR reactions in which the product of the previous reaction was used as the template for the next reaction. The T0 spacer was amplified from plasmid pSR26_2 using primers pCL-F1-up and pCL-tetO1-dn-1. The resulting PCR product was used as the template for a second round of PCR using primers pCL-F1-up and pCL-tetO1-dn-2. The resulting PCR product was used as the template for a third round of PCR using primers pCL-F1-up and pCL-tetO1-dn-3 to generate the final fragment.

The five 5'-UTR-*gfp-uv* fragments were constructed as follows: The pET 5'-UTR-*gfp-uv* fragment was constructed in a single PCR reaction by amplification from plasmid pET101-GFP using primers pCL-GFPuv-up-tetO1 and pCL-F2-dn. The U2 5'-UTR-*gfp-uv*, 26.2 5'-UTR-*gfp-uv*, and pBEST 5'-UTR-*gfp-uv* fragments were each constructed by two sequential PCR reactions in which the product of the first reaction (the *gfp-uv*-containing fragment, which was amplified from plasmid pET101-GFP), was used as the template for the second reaction. The U2 5'-UTR-*gfp-uv* fragment was constructed by amplification using primers pCL-u2-up-1 and pCL-F2-dn; and the resulting PCR product used as the template for a second round of PCR using primers pCL-u2-up-2-tetO1 and pCL-F2-dn. The 26.2 5'-UTR-*gfp-uv* fragment was constructed by amplification using primers pCL-pSR26-up-1 and pCL-F2-dn; and the resulting PCR product used as the template for a second round of PCR using primers pCL-pSR26-up-2-tetO1 and pCL-F2-dn. The pBEST 5'-UTR-*gfp-uv* fragment was constructed by amplification using primers pCL-45784-up-1 and pCL-F2-dn; and the resulting PCR product used as the template for a second round of PCR using primers pCL-45784-up-2-tetO1 and pCL-F2-dn. The BCD2 5'-UTR was constructed as a stand-alone fragment by templateless assembly using three primers (pCL-BCD2-1-tetO1, pCL-BCD2-2, and pCL-BCD2-3). A *gfp-uv*-containing fragment was amplified from pET101-GFP using primers pCL-F2-up-BCD2 and pCL-F2-dn; and the BCD2 5'-UTR and *gfp-uv*-containing fragments were joined by overlap extension PCR and amplified using outside primers pCL-BCD2-1-tetO1 and pCL-F2-dn to generate the final BCD2 5'-UTR-*gfp-uv* fragment. Each of the five 5'-UTR-*gfp-uv* fragment variants was then assembled with the T0 spacer-PLtetO-1, pMB1 origin, and ampicillin resistance marker fragments in a COE-PCR reaction. Each reaction mixture was concentrated using the Zymo Clean and Concentrator Kit and introduced into competent *E.coli* DH5α cells. Each final construct was verified by restriction mapping and sequencing. Primer information is given in the table below. The priming region of each primer is underlined. The vector map of pGBSH1-BCD2 is given as an example. A table summarizing the 5'-UTRs examined is given below.

primer name	**sequence (5' – 3')**	**amplicon size (bp)**	**template**
pCL-F1-up	ACAAACTAGTGCGACCCTGCTGCTTGGATTCTCACCAATAAAAAAC	167	pSR26_2
pCL-tetO1-dn-1	TGTCAATCTCTATCACTGATAGGGATTTGATATCGAGCTCGCTTGGACTCCTGTTGATAG		
pCL-tetO1-dn-2	GCTCAGTATCTCTATCACTGATAGGGATGTCAATCTCTATCACTGATAGGGATTTG	194	PCR pdt.
pCL-tetO1-dn-3	GGTCAGTGCGTCCTGCTGATGTGCTCAGTATCTCTATCACTGATAGGG	216	PCR pdt.
pCL-GFPuv-up-tetO1	ATCAGCAGGACGCACTGACCCCTCTAGAAATAATTTTGTTTAACTTTAAGAAGGAATTC	1071	pET101-GFP
pCL-F2-dn	CCGGGCCTCTTGCGGGATATC (same is used to construct pUC19-GFPuv)		
pCL-u2-up-1	AAAGAGGAGAAAGGTACCATGAGTAAAGGAGAAGAACTTTTCACTGG (used with pCL-F2-dn)	1016	pET101-GFP
pCL-u2-up-2-tetO1	ATCAGCAGGACGCACTGACCGAATTCATTAAAGAGGAGAAAGGTACCATGAG (used with pCL-F2-dn)	1045	PCR pdt.
pCL-pSR26-up-1	AGCAAAGCCCAATTTTAAACAAATGAGTAAAGGAGAAGAACTTTTCACTGG (used with pCL-F2-dn)	1020	pET101-GFP
pCL-pSR26-up-2-tetO1	ATCAGCAGGACGCACTGACCGCATAAAGGACTTAGCAAAGCCCAATTTTAAAC (used with pCL-F2-dn)	1053	PCR pdt.

pCL-45784-up-1	ATTTTGTTTAACTTTAAGAAGGATCCATGAGTAAAGGAGAAGAACTTTTCACTGG (used with pCL-F2-dn)	1024	pET101-GFP
pCL-45784-up-2-tetO1	ATCAGCAGGACGCACTGACCGCTAGCAATAATTTTGTTTAACTTTAAGAAGGATCCATG (used with pCL-F2-dn)	1054	PCR pdt.
pCL-BCD2-1-tetO1	ATCAGCAGGACGCACTGACCGGGCCCAAGTTCACTTAAAAAGGAGATCAAC	125	primer assembly
pCL-BCD2-2	GATTAAGATGTTTCAGTACGAAAATTGCTTTCATTGTTGATCTCCTTTTTAAG		
pCL-BCD2-3	AGTTCTTCTCCTTTACTCATTAGAAAACCTCCTTAGCATGATTAAGATGTTTCAGTAC		
pCL-F2-up-BCD2	ATGAGTAAAGGAGAAGAACTTTTCACTGGAG (used with pCL-F2-dn)	998	pET101-GFP

T0 spacer fragment sequence. Primer binding sites are underlined, and the T0 spacer region is shown in blue.

TGCTTGGATTCTCACCAATAAAAAACGCCCGGCGGCAACCGAGCGTTCTGAACAAATCCAGATGGAGTTCTGAGGTCATTACTGGATCTATCAACAGGAGTCCAAGCGAGCTCGATATCAAAT

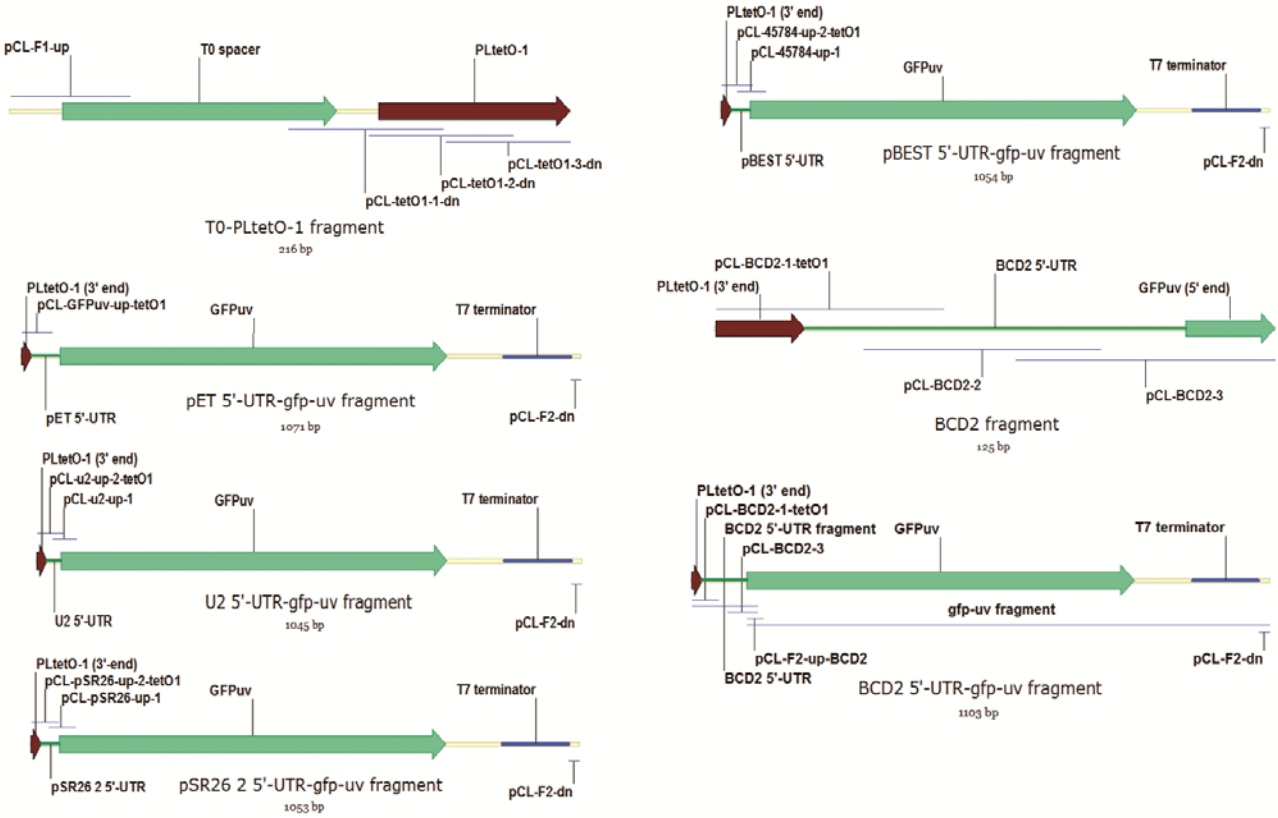

5'-UTR	sequence	length (bp)
pET	CCTCTAGAAATAATTTTGTTTAACTTTAAGAAGGAATTCAGGAGCCCTTCACC	53
U2	GAATTCATTAAAGAGGAGAAAGGTACC	27
26_2	GCATAAAGGACTTAGCAAAGCCCAATTTTAAACAA	35
pBEST	GCTAGCAATAATTTTGTTTAACTTTAAGAAGGATCC	36
BCD2	GGGCCCAAGTTCACTTAAAAAGGAGATCAACAATGAAAGCAATTTTCGTACTGAAACATCTTAATCATGCTAAGGAGGTTTTCTA	85

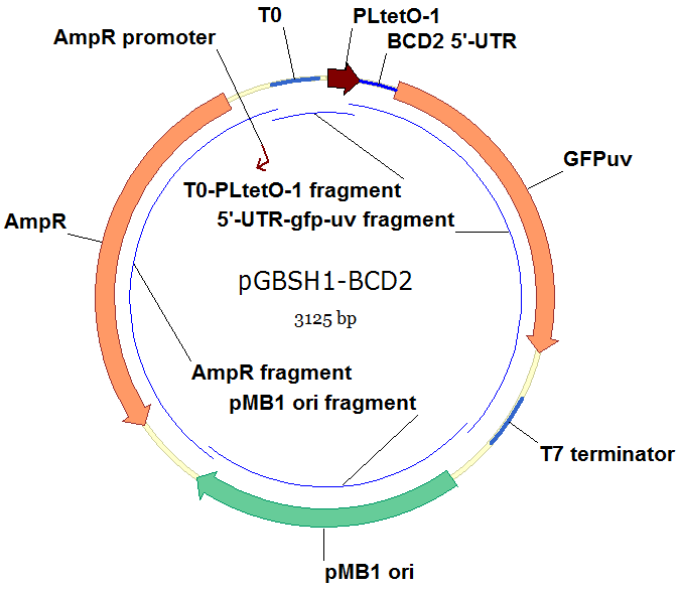

2.3.4. pGBSH1 series functional assay. E. coli DH5α transformed with pGBSH1-BCD2, pGBSH1-U2, pGBSH1-26.2, pGBSH1-pET, and pGBSH1-pBEST displayed a range of fluorescences (Fig. S2) as determined by plate reader fluorescence assays (see cell density and fluorescence assays section, above, for experimental details), with pGBSH1-BCD2 resulting in the highest fluorescence. Thus, pGBSH1-BCD2 was selected for further development.

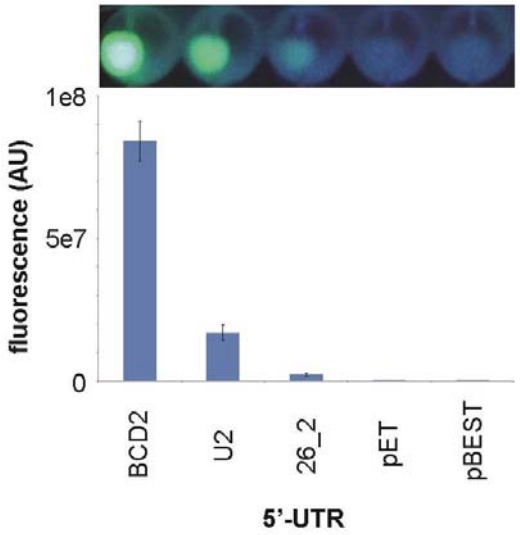

Figure S2. Cell pellet fluorescence and fluorescence quantification of pGBSH1 variants in which the *gfp-uv* 5'-UTR has been altered.

2.3.5. Construction and testing of pGBSH3. After identification of plasmid pGBSH1-BCD2 as the variant resulting in the highest fluorescence, the ampicillin resistance marker in pGBSH1-BCD2 was replaced with a chloramphenicol resistance marker so that the resulting plasmid, pGBSH3, could be co-transformed with pRRSH2-A1408G. A four fragment COE-PCR reaction was employed to construct pGBSH3. Three of the fragments (BCD2 5'-UTR-*gfp-uv*, pMB1 origin, and T0-PLtetO-1) were identical to those used to construct pGBSH1-BCD2. The fragment containing the chloramphenicol resistance marker was amplified from plasmid pBKCM7b (Charles E. Melancon III, unpublished) using primers cat-pBKCM7b-up and cat-pBKCM7b-dn. After COE-PCR, concentration using a Zymo Clean and Concentrator Kit, and transformation, the final construct was verified by restriction mapping and sequencing. Primer information is given in the table below. The priming region of each primer is underlined. Retention of robust fluorescence by *E. coli* DH5α cells transformed with pGBSH3 was verified by plate reader fluorescence assays (Fig. 2b) (see cell density and fluorescence assays section, above, for experimental details).

primer name	sequence (5' – 3')	amplicon size (bp)	template
cat-pBKCM7b-up	CTTTTCTATCTAGACGGGGTCTTTTGATAGAAAATCATAAAAGGATTTGC	1069	pBKCM7b
cat-pBKCM7b-dn	GCAGGGTCGCACTAGTTTGTGGATCCAACTGCATTCAGAATAAATAAATC		

Chloramphenicol resistance marker fragment sequence. Primer binding sites are underlined, the promoter sequence is shown in green, and the chloramphenicol acetyltransferase coding region is shown in blue with start and stop codons underlined.

GGATCCAACTGCATTCAGAATAAATAAATCCTGGTGTCCCTGTTGATACCGGGAAGCCCTGGGCCAACTTTTGGCGAAAATGAGACGTT
GATCGGCACGTAAGAGGTTCCAACTTTCACCATAATGAAATAAGATCACTACCGGGCGTATTTTTTGAGTTGTCGAGATTTTCAGGAGC
TAAGGAAGCTAAAATGGAGAAAAAAATCACTGGATATACCACCGTTGATATATCCCAATGGCATCGTAAAGAACATTTTGAGGCATTTC
AGTCAGTTGCTCAATGTACCTATAACCAGACCGTTCAGCTGGATATTACGGCCTTTTTAAAGACCGTAAAGAAAAATAAGCACAAGTTT
TATCCGGCCTTTATTCACATTCTTGCCCGCCTGATGAATGCTCATCCGGAATTACGTATGGCAATGAAAGACGGTGAGCTGGTGATATG
GGATAGTGTTCACCCTTGTTACACCGTTTTCCATGAGCAAACTGAAACGTTTTCATCGCTCTGGAGTGAATACCACGACGATTTCCGGC
AGTTTCTACACATATATTCGCAAGATGTGGCGTGTTACGGTGAAAACCTGGCCTATTTCCCTAAAGGGTTTATTGAGAATATGTTTTTC
GTCTCAGCCAATCCCTGGGTGAGTTTCACCAGTTTTGATTTAAACGTGGCCAATATGGACAACTTCTTCGCCCCCGTTTTCACCATGGG
CAAATATTATACGCAAGGCGACAAGGTGCTGATGCCGCTGGCGATTCAGGTTCATCATGCCGTTTGTGATGGCTTCCATGTCGGCAGAA
TGCTTAATGAATTACAACAGTACTGCGATGAGTGGCAGGGCGGGGCGTAAGGCGCGCCATTTAAATGAAGTTCCTATTCCGAAGTTCCT
ATTCCTAGGGATTAAAAAGGCAACTTTATGCCCATGCAACAGAAACTATAAAAAATACAGAGAATGAAAAGAAACAGATAGATTTTTTA
GTTCTTTAGGCCCGTAGTCTGCAAATCCTTTTATGATTTTCTATCAAA

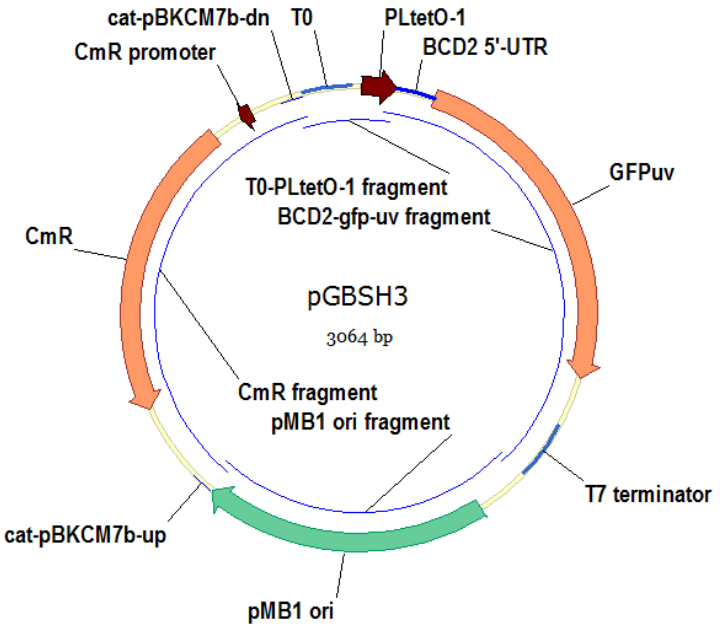

2.3.6. Construction and testing of pGBSH18. A cassette containing the *tetR* gene with orthogonal Shine-Dalgarno (O-SD) sequence (ATCCC)[10, 11] under control of medium strength promoter BBa_J23106 (J. Christopher Anderson, unpublished) and containing the T1 terminator was inserted into pGBSH3 to generate pGBSH18. A five fragment COE-PCR reaction was employed to construct pGBSH18. Three of the fragments (the BCD2 5'-UTR-*gfp-uv*, chloramphenicol resistance marker, and T0-PLtetO-1) were identical to those used to construct pGBSH1-BCD2 and pGBSH3. The pMB1 origin was amplified from pGBSH3 using primers F3-up-tetRassem and pCL-F3-pMB1-dn.

The fragment containing O-SD-*tetR* was constructed by three sequential PCR reactions in which the product of the previous reaction was used as the template for the next reaction. The *tetR* gene with T1 terminator was amplified from pSR26_2 using primers ptetR-1-KF-up and tetRassem1-dn-XmnI. The resulting PCR product was used as the template for a second round of PCR using primers ptetR-2-KF-up and tetRassem1-dn-XmnI. The resulting PCR product was used as the template for a third round of PCR using primers tetRassem1-up-XmnI and tetRassem1-dn-XmnI to generate the final fragment. After COE-PCR, concentration using a Zymo Clean and Concentrator Kit, and transformation, the final construct was verified by restriction mapping and sequencing. Primer information is given in the table below. The priming region of each primer is underlined. The O-SD sequence and ATG start codon are shown in bold red in the primers that contain them. Retention of robust fluorescence by *E. coli* cells DH5α transformed with pGBSH18 was verified as by plate reader fluorescence assays (Fig. 2b) (see cell density and fluorescence assays section, above, for experimental details). During the sequencing process, we discovered two spontaneous mutations in the pMB1 origin (see below for locations). It is unclear whether these mutations have any effect on plasmid copy number, but it is clear from fluorescence assays that they do not interfere with replication in *E. coli* DH5α or *gfp-uv* expression.

primer name	sequence (5' – 3')	amplicon size (bp)	template
F3-up-tetRassem	GCGGTAATAAGCTTACGGTTATCCAC	738	pGBSH3
pCL-F3-pMB1-dn	AGACCCCGTCTAGATAGAAAAGATCAAAGGATCTTCTTGAG (same as used to construct pUC19-GFPuv)		
ptetR-1-KF-up	ACAATCGATA**CATCCC**CCGCAA**ATG**ATGTCTCGTTTAGATAAAAGTAAAG	823	pSR26_2
tetRassem1-dn-XmnI	TGTGGATAACCGTAAGCTTATTACCGCTTTGAGTGAGCTGATACCGC		
ptetR-2-KF-up	CTAGCTCAGTCCTAGGTATAGTGCTAGCCCAGCCAGAGAAACAATCGATA**CATCCC**CC	863	PCR pdt.
tetRassem1-up-XmnI	ATATCCCGCAAGAGGCCCGGTTTACGGCTAGCTCAGTCCTAG	890	PCR pdt.

Sequence of the tetR-T1 terminator fragment. Primer binding sites are underlined, the *tetR* coding sequence is shown in blue, and the T1 terminator region is shown in green.

ATGATGTCTCGTTTAGATAAAAGTAAAGTGATTAACAGCGCATTAGAGCTGCTTAATGAGGTCGGAATCGAAGGTTTAACAACCCGTAA
ACTCGCCCAGAAGCTAGGTGTAGAGCAGCCTACATTGTATTGGCATGTAAAAAATAAGCGGGCTTTGCTCGACGCCTTAGCCATTGAGA
TGTTAGATAGGCACCATACTCACTTTTGCCCTTTAGAAGGGGAAAGCTGGCAAGATTTTTTACGTAATAACGCTAAAAGTTTTAGATGT
GCTTTACTAAGTCATCGCGATGGAGCAAAAGTACATTTAGGTACACGGCCTACAGAAAAACAGTATGAAACTCTCGAAAATCAATTAGC
CTTTTTATGCCAACAAGGTTTTTCACTAGAGAATGCATTATATGCACTCAGCGCAGTGGGGCATTTTACTTTAGGTTGCGTATTGGAAG
ATCAAGAGCATCAAGTCGCTAAAGAAGAAAGGGAAACACCTACTACTGATAGTATGCCGCCATTATTACGACAAGCTATCGAATTATTT
GATCACCAAGGTGCAGAGCCAGCCTTCTTATTCGGCCTTGAATTGATCATATGCGGATTAGAAAAACAACTTAAATGTGAAAGTGGGTC
TTAAGGCATCAAATAAAACGAAAGGCTCAGTCGAAAGACTGGGCCTTTCGTTTTATCTGTTGTTTGTCGGTGAACGCTCTCCTGAGTAG
GACAAATCCGCCGCCCTAGACCTAGGCGTTCGGCTGCGGCGAGCGGTATCAGCTCACTCAAAG

Sequence of the pMB1 origin in pGBSH18 with spontaneous mutations marked in bold underlined red. G at position 107 was mutated to C, and G at position 457 was mutated to A.

CGCGTTGCTGGCGTTTTTCCATAGGCTCCGCCCCCCTGACGAGCATCACAAAAATCGACGCTCAAGTCAGAGGTGGCGAAACCCGACAG
GACTATAAAGATACCAG**C**CGTTTCCCCCTGGAAGCTCCCTCGTGCGCTCTCCTGTTCCGACCCTGCCGCTTACCGGATACCTGTCCGCC
TTTCTCCCTTCGGGAAGCGTGGCGCTTTCTCATAGCTCACGCTGTAGGTATCTCAGTTCGGTGTAGGTCGTTCGCTCCAAGCTGGGCTG
TGTGCACGAACCCCCCGTTCAGCCCGACCGCTGCGCCTTATCCGGTAACTATCGTCTTGAGTCCAACCCGGTAAGACACGACTTATCGC
CACTGGCAGCAGCCACTGGTAACAGGATTAGCAGAGCGAGGTATGTAGGCGGTGCTACAGAGTTCTTGAAGTGGTGGCCTAACTACGGC

TACACTAGAAGAACAGTATTTGGTATCTGCGCTCTGCTGAAGCCAGTTACCTTCGGAAAAAGAGTTGGTAGCTCTTGATCCGGCAAACA
AACCACCGCTGGTAGCGGTGGTTTTTTTGTTTGCAAGCAGCAGATTACGCGCAGAAAAAAAGGATCTCAAGAAGATCCTTT

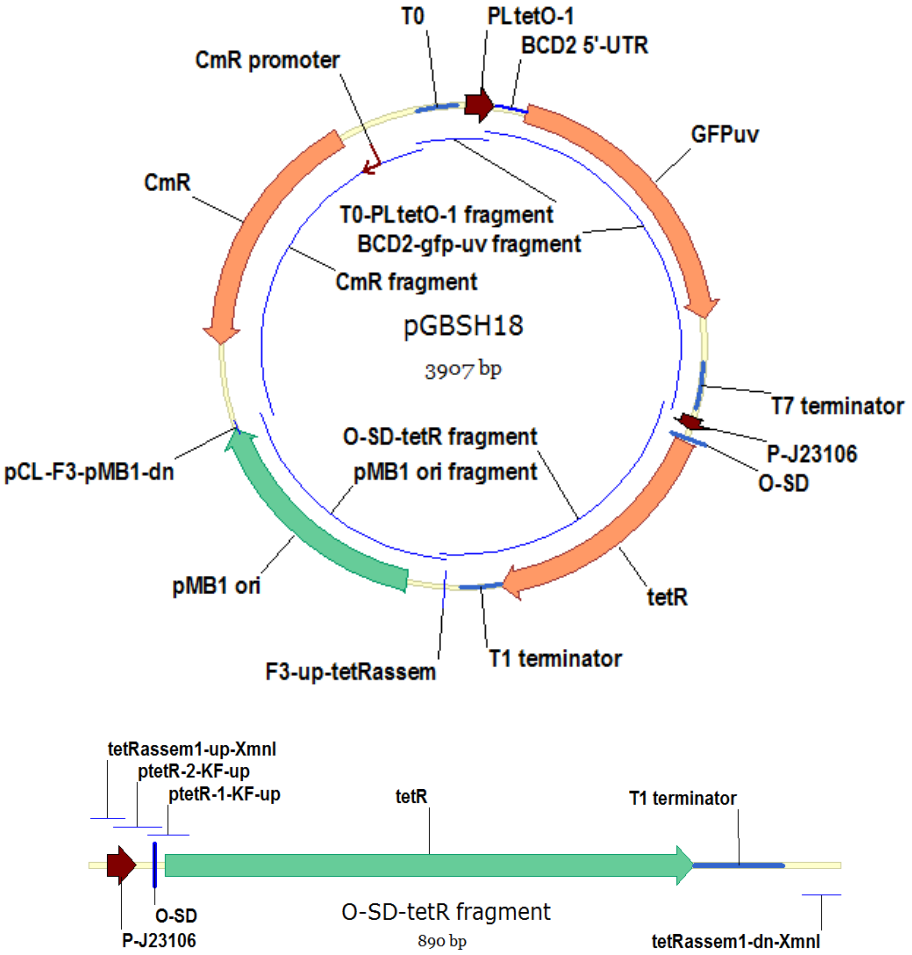

2.3.7. Construction and testing of pSH3-KF in E. coli DH5α. A cassette containing the orthogonal 16S rRNA (O-16S) with orthogonal anti-Shine-Dalgarno (O-ASD) sequence (TGGGG)[10, 11] was inserted into pGBSH18 to generate pSH3-KF, which contains all the components of the orthogonal ribosome-based fluorescent reporter. A five fragment COE-PCR reaction was employed to construct pSH3-KF.

Two of the fragments (the O-SD-*tetR* and pMB1 origin) were identical to those used to construct pGBSH18. The chloramphenicol resistance marker fragment was amplified from pBGSH18 using primers cat-pBKCM7b-up and pCAT-OKF-dn. A fragment containing T0-PLtetO-1 and BCD2 5'-UTR-*gfp*-uv was also amplified from pGBSH18 using primers pGFP-OKF-up and pCL-F2-dn.

The fragment containing the orthogonal 16S rRNA (O-16S) under control of the reportedly strong *lpp* promoter (Plpp)[12] was constructed by amplifying the Plpp-16S rRNA cassette from plasmid pTrcSS1d-rrsBb (Shinichiro Shoji, unpublished) using upstream primer pO16S-up and mutagenic downstream primer pO16S-KF-dn which was used to install the orthogonal anti-Shine-Dalgarno (O-ASD) sequence. The strong terminator BBa_B0015[13] was amplified from plasmid pSR26_2 using primers pB15-up and pB15-dn and appended to the 3' end of the Plpp-O-16S fragment by overlap extension PCR to attempt to minimize any polar effects on other genes in the construct. After COE-PCR, concentration using a Zymo Clean and Concentrator Kit, and transformation, the final construct was verified by restriction mapping and sequencing. Primer information is given in the table below. The priming region of each primer is underlined. The *lpp* promoter and O-ASD sequences are shown in bold red in the primers that contain them.

As expected, a nearly complete lack of fluorescence by *E. coli* DH5α cells transformed with pSH3-KF was observed (Fig. 2b) as determined by plate reader fluorescence assays (see cell density and fluorescence assays section,

above, for experimental details). However, as expected, fluorescence of *E. coli* DH5α cells transformed with pSH3-KF could be recovered in a dose-dependent manner by addition of various concentrations of anhydrotetracycline (ATC), which binds to TetR and causes its dissociation from PLtetO-1 thereby relieving repression of transcription (Fig. S3).

primer name	sequence (5' – 3')	amplicon size (bp)	template
pGFP-OKF-up	GAATTCGTGGCCCTGCATGCACAAACTAGTGCGACCCTGCTGC	1319	pGBSH18
pCL-F2-dn	CCGGGCCTCTTGCGGGATATC (same is used to construct pUC19-GFPuv)		
cat-pBKCM7b-up	CTTTTCTATCTAGACGGGGTCTTTTGATAGAAAATCATAAAAGGATTTGC (same as used to construct pGBSH3)	1091	pGBSH18
pCAT-OKF-dn	GTACCCGTGGATCCTCTAGAGGATCCAACTGCATTCAGAATAAATAAATC		
pO16S-up	GCATGCAGGGCCACGAA**TTCTCAACATAAAAAACTTTGTGTAATACT**TGTAACGCTAGATCCGGTAGCGATCGAAAGCGAAGCGGCAC	1824	pTrcSS1d-rrsBb
pO16S-KF-dn	CTGCAGTATCAGACAATCTGTGTGAGCACTACAAAGTACGCTTCTTTAAGGTA**CCCCA**TGATCCAACCG		
pB15-up	CAGATTGTCTGATACTGCAGGCATGATAATAATCTAGACCAGG	188	pSR26_2
pB15-dn	TCTAGAGGATCCACGGGTACC		

Sequence of the *lpp* promoter - O16S fragment. Primer binding sites are underlined, the *lpp* promoter is shown in green, the O-16S rRNA coding region is shown in blue, and the O-ASD sequence is shown in red.

ATTCTCAACATAAAAAACTTTGTGTAATACTTGTAACGCTAGATCCGGTAGCGATCGAAAGCGAAGCGGCACTGCTCTTTAACAATTTA
TCAGACAATCTGTGTGGGCACTCGAAGATACGGATTCTTAACGTCGCAAGACGAAAAATGAATACCAAGTCTCAAGAGTGAACACGTAA
TTCATTACGAAGTTTAATTCTTTGAGCGTCAAACTTTTAAATTGAAGAGTTTGATCATGGCTCAGATTGAACGCTGGCGGCAGGCCTAA
CACATGCAAGTCGAACGGTAACAGGAAGAAGCTTGCTTCTTTGCTGACGAGTGGCGGACGGGTGAGTAATGTCTGGGAAACTGCCTGAT
GGAGGGGGATAACTACTGGAAACGGTAGCTAATACCGCATAACGTCGCAAGACCAAAGAGGGGGACCTTCGGGCCTCTTGCCATCGGAT
GTGCCCAGATGGGATTAGCTAGTAGGTGGGGTAACGGCTCACCTAGGCGACGATCCCTAGCTGGTCTGAGAGGATGACCAGCCACACTG
GAACTGAGACACGGTCCAGACTCCTACGGGAGGCAGCAGTGGGGAATATTGCACAATGGGCGCAAGCCTGATGCAGCCATGCCGCGTGT
ATGAAGAAGGCCTTCGGGTTGTAAAGTACTTTCAGCGGGGAGGAAGGGAGTAAAGTTAATACCTTTGCTCATTGACGTTACCCGCAGAA
GAAGCACCGGCTAACTCCGTGCCAGCAGCCGCGGTAATACGGAGGGTGCAAGCGTTAATCGGAATTACTGGGCGTAAAGCGCACGCAGG
CGGTTTGTTAAGTCAGATGTGAAATCCCCGGGCTCAACCTGGGAACTGCATCTGATACTGGCAAGCTTGAGTCTCGTAGAGGGGGGTAG
AATTCCAGGTGTAGCGGTGAAATGCGTAGAGATCTGGAGGAATACCGGTGGCGAAGGCGGCCCCCTGGACGAAGACTGACGCTCAGGTG
CGAAAGCGTGGGGAGCAAACAGGATTAGATACCCTGGTAGTCCACGCCGTAAACGATGTCGACTTGGAGGTTGTGCCCTTGAGGCGTGG
CTTCCGGAGCTAACGCGTTAAGTCGACCGCCTGGGGAGTACGGCCGCAAGGTTAAAACTCAAATGAATTGACGGGGGCCCGCACAAGCG
GTGGAGCATGTGGTTTAATTCGATGCAACGCGAAGAACCTTACCTGGTCTTGACATCCACGGAAGTTTTCAGAGATGAGAATGTGCCTT
CGGGAACCGTGAGACAGGTGCTGCATGGCTGTCGTCAGCTCGTGTTGTGAAATGTTGGGTTAAGTCCCGCAACGAGCGCAACCCTTATC
CTTTGTTGCCAGCGGTCCGGCCGGGAACTCAAAGGAGACTGCCAGTGATAAACTGGAGGAAGGTGGGGATGACGTCAAGTCATCATGGC
CCTTACGACCAGGGCTACACACGTGCTACAATGGCGCATACAAAGAGAAGCGACCTCGCGAGAGCAAGCGGACCTCATAAAGTGCGTCG
TAGTCCGGATTGGAGTCTGCAACTCGACTCCATGAAGTCGGAATCGCTAGTAATCGTGGATCAGAATGCCACGGTGAATACGTTCCCGG
GCCTTGTACACACCGCCCGTCACACCATGGGAGTGGGTTGCAAAAGAAGTAGGTAGCTTAACCTTCGGGAGGGCGCTTACCACTTTGTG
ATTCATGACTGGGGTGAAGTCGTAACAAGGTAACCGTAGGGGAACCTGCGGTTGGATCATGGGGTACCTTAAAGAAGCGTACTTTGTAG
TGCTCACACAGATTGTCTGATA

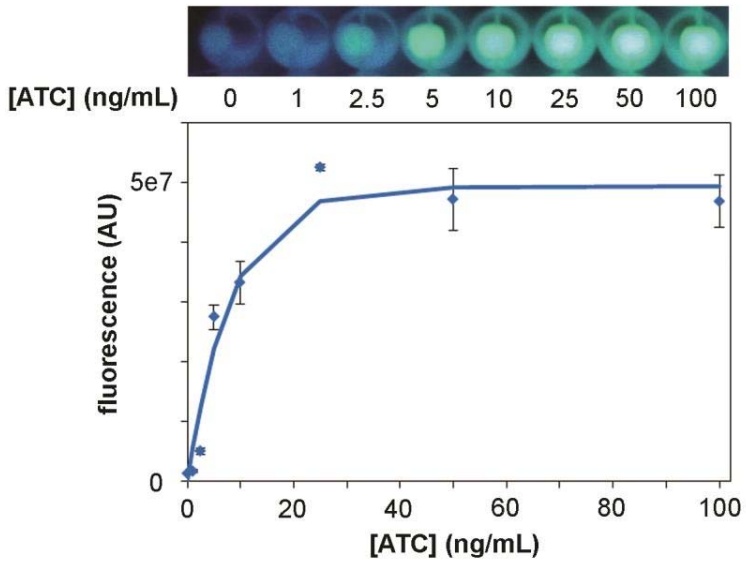

Figure S3. Cell pellet fluorescence and fluorescence quantification of *E. coli* **DH5α** cells containing pSH3-KF grown in the presence of a range of anhydrotetracycline concentrations.

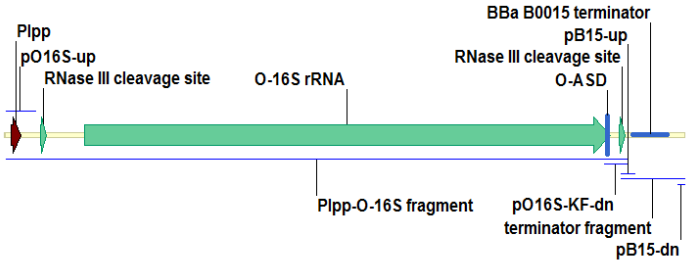

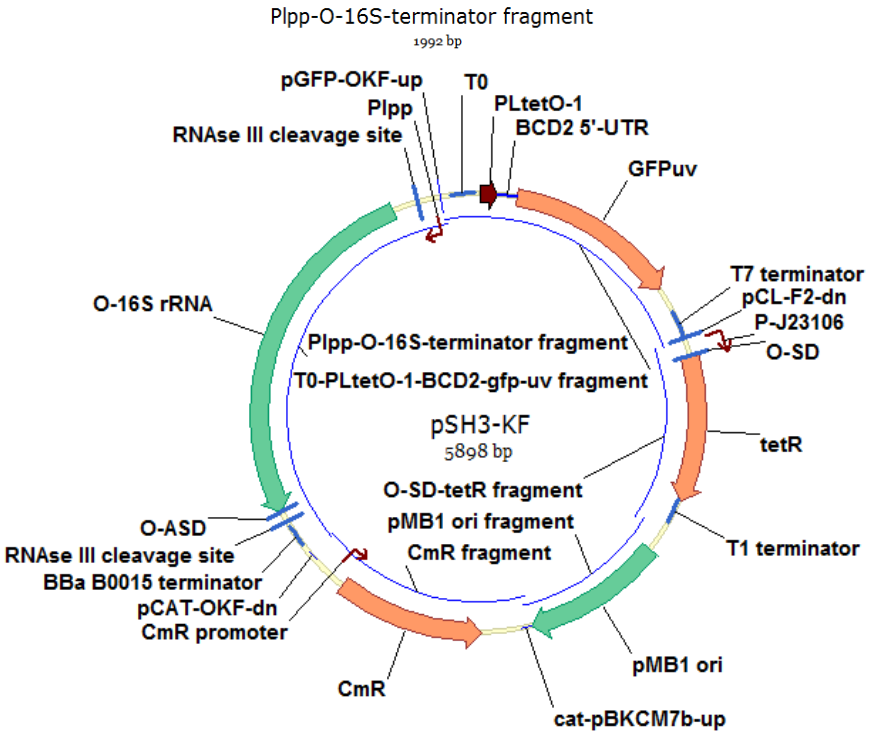

2.4. Ribosome inhibition assays using pSH series plasmids in E. coli SH386 and SH424.

2.4.1. Ribosome inhibition assay of kanamycin in E. coli SH391. We tested the ability of *E. coli* SH386 cells transformed with pSH3-KF (referred to as *E. coli* SH391) to detect ribosome inhibition by kanamycin. *E. coli* SH391 cells were grown in the presence of various concentrations of kanamycin ranging from 0-500 μM and analyzed by fluorescence assay (see Section 1.6 for experimental details). *E. coli* SH391 displayed strong fluorescence in the absence of kanamycin and only a modest (~50%) increase in fluorescence when kanamycin was added (Fig. 3, main text). This result led us to construct and test plasmids pSH4-KF – pSH14-KF in *E. coli* SH386.

2.4.2. Construction and testing of pSH4-KF - pSH14-KF in E. coli SH386. To attempt to overcome the low sensitivity to kanamycin and high background fluorescence imparted by pSH3-KF in *E. coli* SH386 (see Fig. 3 in main text), we constructed a series of eleven pSH3-KF variants in which the strengths of the two promoters controlling expression of *tetR* and O-16S rRNA were combinatorially altered using synthetic constitutive promoters with characterized strengths (J. Christopher Anderson, unpublished,). In addition to the original medium strength synthetic promoter BBa_J23106 controlling *tetR* expression, strong promoter BBa_J23100 and weak promoter BBa_J23115 were selected for use with *tetR*. In addition to the original *lpp* promoter controlling O-16S rRNA expression, strong promoter BBa_J23100, medium strength promoter BBa_J23108, and weak strength promoter BBa_J23114 were selected for use with O-16S rRNA.

We first constructed two plasmids, pSH4-KF and pSH5-KF, in which the BBa_J23106 promoter controlling expression of *tetR* was replaced with strong promoter BBa_J23100 and a weak promoter BBa_J23115, respectively. Promoter replacement was accomplished by overlap extension PCR of two fragments amplified from pSH3-KF whose junction encompassed each promoter to be inserted, digestion of both the resulting PCR product and pSH3-KF with unique restriction sites MfeI and NdeI, and ligation of the PCR product into the vector. For construction of pSH4-KF, primer pSH4-KF-1 and mutagenic primer pSH4-KF-2 were used to amplify fragment 1; and mutagenic primer pSH4-KF-3 and primer pSH4-KF-4 were used to amplify fragment 2. For construction of pSH5-KF, primer pSH4-KF-1 and mutagenic primer pSH5-KF-2 were used to amplify fragment 1; and mutagenic primer pSH5-KF-3 and primer pSH4-KF-4 were used to amplify fragment 2. Plasmids pSH4-KF and pSH5-KF were verified by sequencing the cloned region. Primer information is given in the table below. The priming region of each primer is underlined.

To construct the remaining nine plasmid variants bearing strong (pSH6-KF, pSH9-KF, pSH12-KF), medium (pSH7-KF, pSH10-KF, pSH13-KF), and weak (pSH8-KF, pSH11-KF, pSH14-KF) strength promoters controlling expression of O-16S, we used a similar overlap extension PCR strategy. Two fragments amplified from pSH3-KF whose junction encompassed each promoter to be inserted were joined by overlap extension PCR. The PCR product bearing strong promoter BBa_J23100 was constructed using primer pSH6-KF-1 and mutagenic primer pSH6-KF-2 to amplify fragment 1; and mutagenic primer pSH6-KF-3 and primer pSH6-KF-4 to amplify fragment 2. The PCR product bearing medium promoter BBa_J23108 was constructed using primer pSH6-KF-1 and mutagenic primer pSH7-KF-2 to amplify fragment 1; and mutagenic primer pSH7-KF-3 and primer pSH6-KF-4 to amplify fragment 2. The PCR product bearing weak promoter BBa_J23114 was constructed using primer pSH6-KF-1 and mutagenic primer pSH8-KF-2 to amplify fragment 1; and mutagenic primer pSH8-KF-3 and primer pSH6-KF-4 to amplify fragment 2. Each of the resulting three PCR products was digested with unique restriction enzymes PstI and SpeI and ligated into each pSH3-KF, pSH4-KF, and pSH5-KF digested with the same enzymes to generate the nine final constructs pSH6-KF through pSH14-KF. All nine plasmids were verified by sequencing the cloned region. Primer information is given in the table below. The priming region of each primer is underlined. Regions of the mutagenic primers containing promoter regions are show in bold red. Diagrams of pSH4-KF and pSH6-KF are shown as examples. Summaries of the names, sequences, and strengths (as measured by J. Christopher Anderson, unpublished) of the promoters used and of the *tetR* and O-16S promoters found in each plasmid are summarized in two tables below. *E. coli* SH386 cells transformed with pSH4-KF – pSH14-KF displayed a range of kanamycin concentration-dependent fluorescent phenotypes as determined by plate reader fluorescence assays (see cell density and fluorescence assays section, above, for experimental details). *E. coli* SH386 cells transformed with pSH6-KF (referred to as *E. coli* SH391) displayed the most favorable properties: essentially no background fluorescence in the absence of kanamycin, and a robust dose-dependent increase in fluorescence in response to kanamycin (Fig. 3). Thus, *E. coli* SH391 was selected for subsequent experiments. Interestingly, the results are consistent with the *lpp* promoter being the weakest of the six promoters tested. The full fluorescence quantification data are shown in Fig. S4.

primer name	sequence (5' – 3')	amplicon size (bp)	template
pSH4-KF-1	ACGGGAACTACAAGACGCGTGCTG	725	pSH3-KF
pSH4-KF-2	**GCTAGCACTGTACCTAGGACTGAGCTAGCCGTCAA**CCGGGCCTCTTGCGGG		
pSH4-KF-3	**CAGTCCTAGGTACAGTGCTAGC**CCAGCCAGAG	769	pSH3-KF
pSH4-KF-4	CCTACTCAGGAGAGCGTTCACCG		
pSH5-KF-2	**GCTAGCATTGTACCTAGGACTGAGCTAGCTATAAA**CCGGGCCTCTTGCGGG (used with pSH4-KF-1)	725	pSH3-KF
pSH5-KF-3	**CAGTCCTAGGTACAATGCTAGC**CCAGCCAGAG (used with pSH4-KF-4)	769	pSH3-KF
pSH6-KF-1	GTGACTCTAGTAGAGAGCGTTCACCGAC	1926	pSH3-KF
pSH6-KF-2	**TTGACGGCTAGCTCAGTCCTAGGTACAGTGCTAGC**TACTTGTAACGCTAGATCCGG		
pSH6-KF-3	**AGGACTGAGCTAGCCGTCAA**TCGTGGCCCTGCATGCAC	375	pSH3-KF
pSH6-KF-4	GGGACAACTCCAGTGAAAAGTTCTTCTCC		
pSH7-KF-2	**CTGACAGCTAGCTCAGTCCTAGGTATAATGCTAGC**TACTTGTAACGCTAGATCCGG (used with pSH6-KF-1)	1926	pSH3-KF
pSH7-KF-3	**AGGACTGAGCTAGCCATAAA**TCGTGGCCCTGCATGCAC (used with pSH6-KF-4)	375	pSH3-KF
pSH8-KF-2	**TTTATGGCTAGCTCAGTCCTAGGTACAATGCTAGC**TACTTGTAACGCTAGATCCGG (used with pSH6-KF-1)	1926	pSH3-KF
pSH8-KF-3	**AGGACTGAGCTAGCCATAAA**TCGTGGCCCTGCATGCAC (used with pSH6-KF-4)	375	pSH3-KF

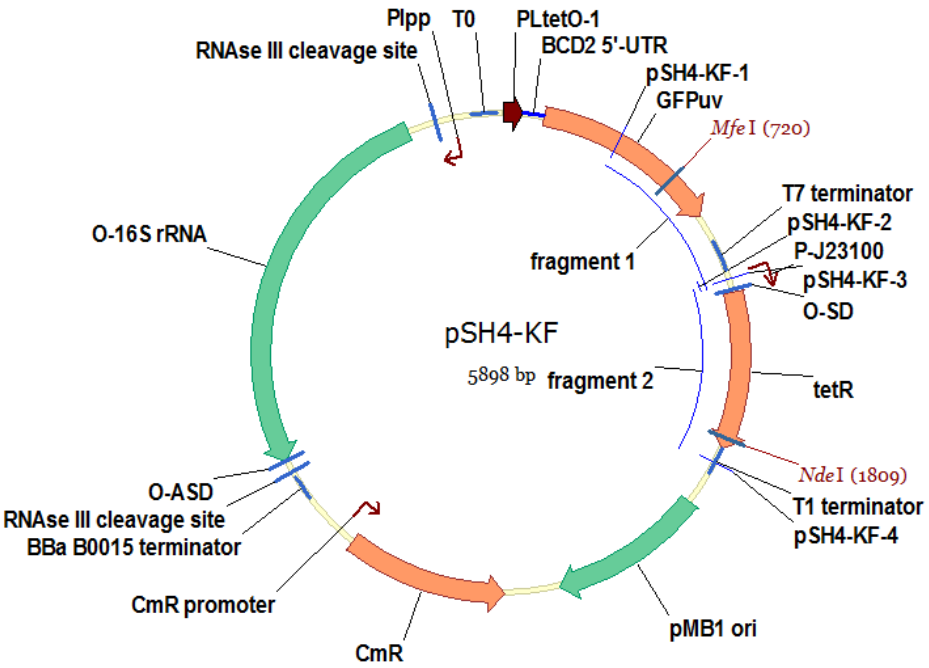

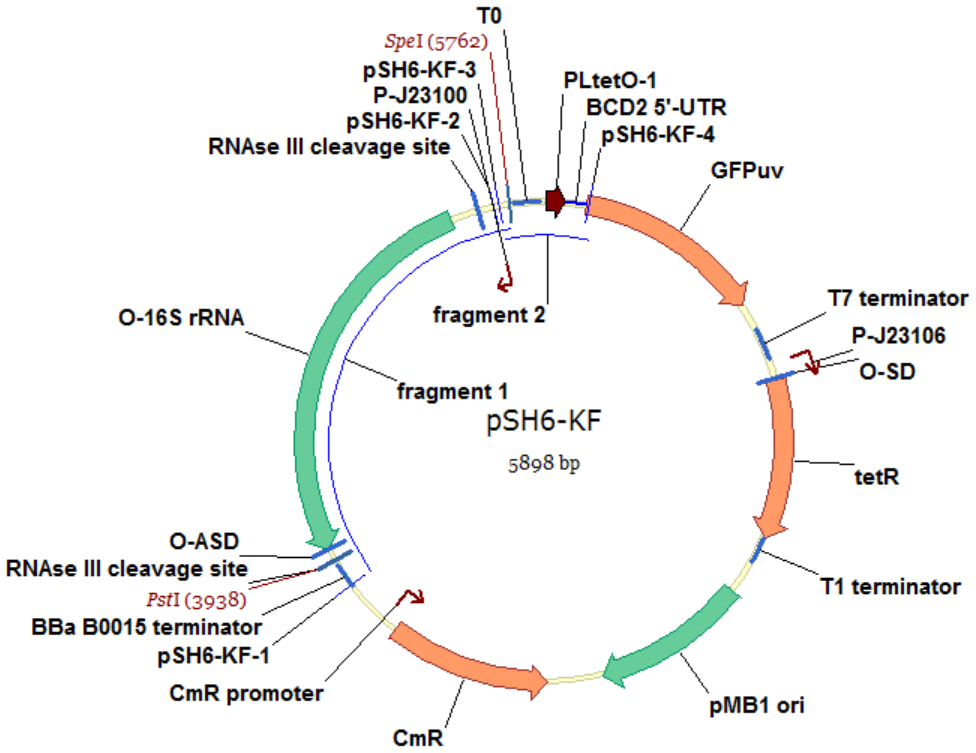

Name	Sequence	Strength
BBa_J23100	**TTGACG**GCTAGCTCAGTCCTAGG**TACAGT**GCTAGC	Strong (1.0)
BBa_J23106	**TTTACG**GCTAGCTCAGTCCTAGG**TATAGT**GCTAGC	Medium (0.47)
BBa_J23115	**TTTATA**GCTAGCTCAGCCCTTGG**TACAAT**GCTAGC	Weak (0.15)
BBa_J23108	**CTGACA**GCTAGCTCAGTCCTAGG**TATAAT**GCTAGC	Medium (0.51)
BBa_J23114	**TTTATG**GCTAGCTCAGTCCTAGG**TACAAT**GCTAGC	Weak (0.10)
lpp	**TTCTCA**ACATAAAAAACTTTGTGT**AATACT**	

	tetR		O-16S	
plasmid	**promoter**	**strength**	**promoter**	**strength**
pSH3-KF	BBa_J23106	Medium (0.47)	lpp	ND
pSH4-KF	BBa_J23100	Strong (1.0)	lpp	ND
pSH5-KF	BBa_J23115	Weak (0.15)	lpp	ND
pSH6-KF	BBa_J23106	Medium (0.47)	BBa_J23100	Strong (1.0)
pSH7-KF	BBa_J23106	Medium (0.47)	BBa_J23108	Medium (0.51)
pSH8-KF	BBa_J23106	Medium (0.47)	BBa_J23114	Weak (0.10)
pSH9-KF	BBa_J23100	Strong (1.0)	BBa_J23100	Strong (1.0)
pSH10-KF	BBa_J23100	Strong (1.0)	BBa_J23108	Medium (0.51)
pSH11-KF	BBa_J23100	Strong (1.0)	BBa_J23114	Weak (0.10)
pSH12-KF	BBa_J23115	Weak (0.15)	BBa_J23100	Strong (1.0)
pSH13-KF	BBa_J23115	Weak (0.15)	BBa_J23108	Medium (0.51)
pSH14-KF	BBa_J23115	Weak (0.15)	BBa_J23114	Weak (0.10)

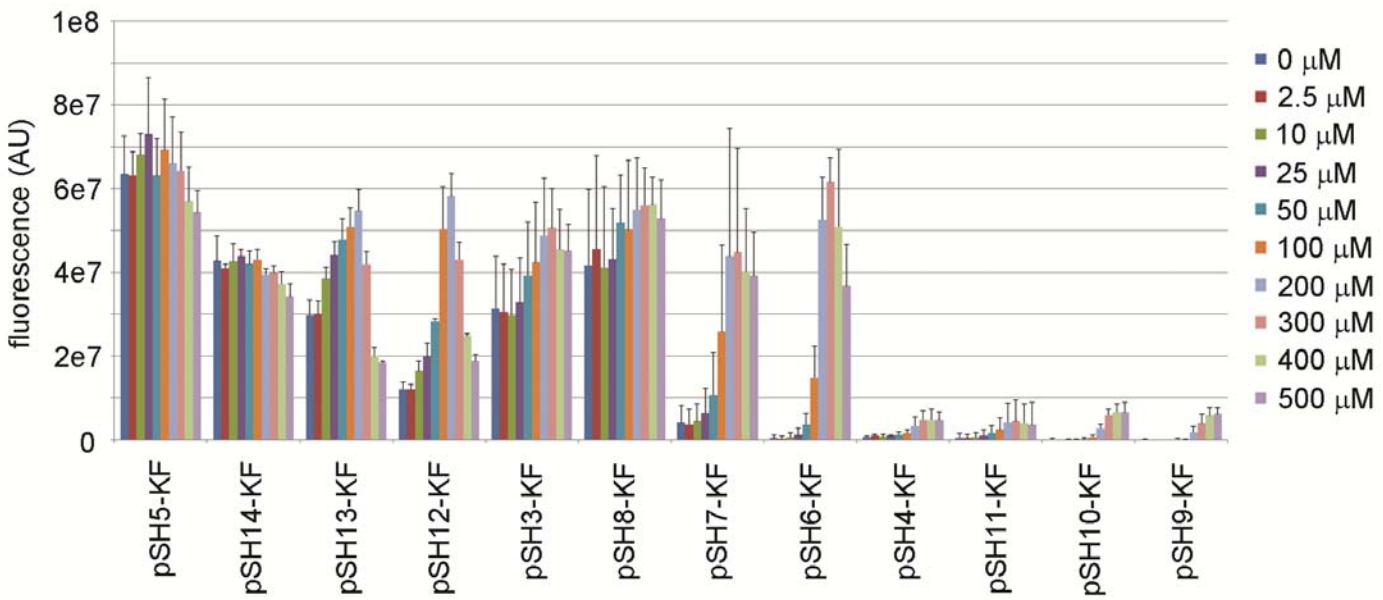

Figure S4. Fluorescence quantification of *E. coli* SH386 cells containing pSH3-KF – pSH14-KF grown in the presence of a range of kanamycin concentrations.

2.4.3. Ribosome inhibition assays of aminoglycosides in E. coli SH399 and SH431. E. coli SH399, which harbors detection plasmid pSH6-KF, was used to conduct ribosome inhibition assays using a range of concentrations of twelve structurally diverse aminoglycosides – kanamycin, apramycin, neomycin, paromomycin, gentamicin, amikacin, neamine, ribostamycin, sisomicin, tobramycin, geneticin (G418), and hygromycin – over a range of nineteen drug concentrations. We observed dose-dependent fluorescence responses by *E. coli* SH399 when treated with ten of these compounds as determined by plate reader fluorescence assays (see section 1.6 for experimental details). See main text and Fig. 4a for additional explanation and data, Fig. S5 for full fluorescence and cell density quantification data, and Fig. S6 for analysis of the correlations between IC_{50} values determined from fluorescence data (see section 1.7 for details on how IC_{50} values were determined) and IC_{50} values previously determined through *in vitro* translation assays (main text, ref. 28). To extend the approach to a system with a different aminoglycoside resistance mutation, we replaced prrnC-sacB with pRRSH2-U1406A (see Section 2.2.2 for vector construction) in *E. coli* SQ380 and then transformed the resulting strain *E. coli* SH424 with pSH6-KF, resulting in the detection strain *E. coli* SH431. *E. coli* SH431 was used to conduct ribosome inhibition assays identical to those performed with *E. coli* SH399. We observed dose-dependent fluorescence responses by *E. coli* SH431 when treated with four of these compounds as determined by plate reader fluorescence assays (see section 1.6 for experimental details), including two to which *E. coli* SH399 was not resistant and therefore could not produce a response. See main text and Fig. 4b for additional explanation and data, Fig. S7 for full fluorescence and cell density quantification data.

2.4.4. Growth inhibition assays of aminoglycosides in E. coli SH434. We constructed *E. coli* SH434, which harbors pRRSH2 (wild-type 16S rRNA, see Section 2.2.2 for vector construction and Section 2.2.3 for functional testing) and pSH6-KF, and used it as a control strain to compare the potencies of the twelve aminoglycosides in a growth inhibition assay and to check for innate resistance on the part of *E. coli* SQ380 to any of the aminoglycosides tested. We examined the growth of *E. coli* SH434 in the presence of a range of concentrations of each aminoglycoside (Fig. S5, S7). See Fig. S6, S8 for analysis of the correlations between IC_{50} values determined from fluorescence data and LD_{50} values determined from these growth inhibition assays. See section 1.7 for details on how IC_{50} and LD_{50} values were determined. *E. coli* SH434 did not display innate resistance to any of the compounds except moderately to hygromycin. However, this did not prevent detection of ribosome inhibition by hygromycin in SH431.

Figure S5. Fluorescence quantification (top row of graphs) and OD_{600} quantification (middle row of graphs) of *E. coli* SH399 (pSH6-KF, pRRSH2-A1408G) cells grown in a range of concentrations (0-500 μM) of each of the twelve aminoglycosides examined; and OD_{600} quantification (bottom row of graphs) of *E. coli* SH434 (pSH6-KF, pRRSH2) cells grown in a range of concentrations (0-32 or 0-1024 μM, 2-fold serial dilutions) of each of the twelve aminoglycosides examined. The scale of x and y axes is consistent for each row of bar charts. Further discussion of these results is presented in the main article.

AMG	IC_{50} (nM) (main text, ref 28)	IC50 (uM)
Gen	20	10.8
Neo	28	12.5
Paro	40	25.5
Tob	50	26.2
Rib	100	89.0
Kan	150	183.0

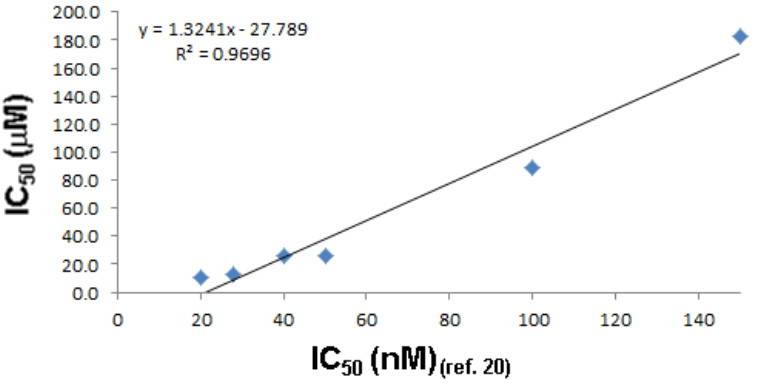

AMG	LD_{50} (uM)	IC_{50} (uM)
Sis	1.8	5.2
Tob	2.7	26.2
Gen	2.9	10.8
Ami	3.0	32.6
Rib	6.8	89.0
Apr	9.7	177.0

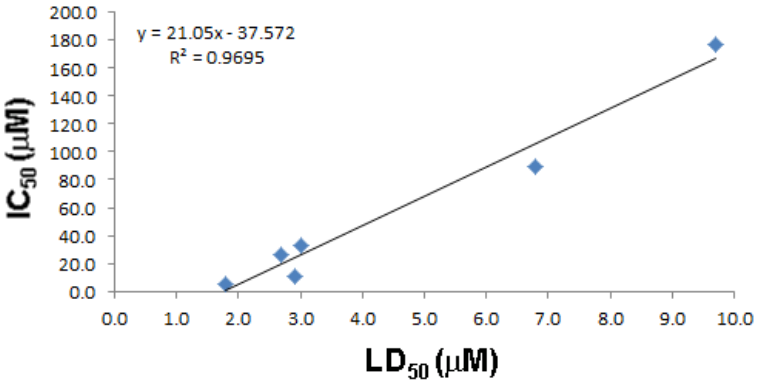

AMG	LD_{50} (uM)	IC_{50} (uM)
Sis	1.8	5.2
Tob	2.7	26.2
Gen	2.9	10.8
Ami	3.0	32.6
Neo	5.3	12.5
Kan	5.5	183.0
Rib	6.8	89.0
Paro	7.8	25.5
Apr	9.7	177.0
Nea	45.5	ND

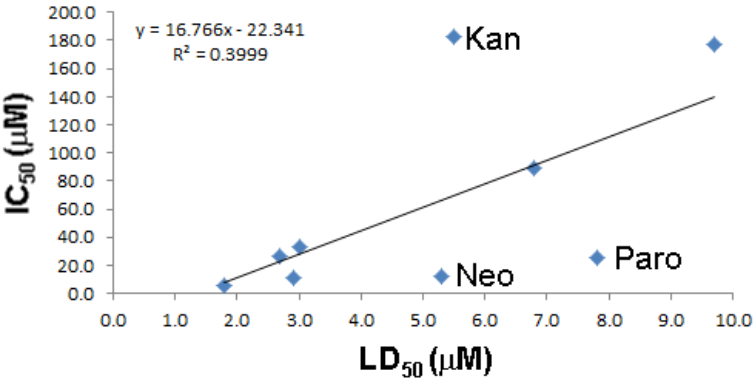

Figure S6. Analysis of the correlations between: (top table and graph) IC_{50} values previously determined through *in vitro* translation assays (main text, ref. 28) (column 1, x axis) and IC_{50} values determined from *E. coli* SH399-derived fluorescence data (column 2, y axis); (middle table and graph) LD_{50} values determined from growth inhibition assays of *E. coli* SH434 (column 1, x axis) and IC_{50} values determined from *E. coli* SH399-derived fluorescence data for the subset of 6 compounds for which there was a statistically significant correlation (column 2, y axis); and (bottom table and graph) LD_{50} values determined from growth inhibition assays of *E. coli* SH434 (column 1, x axis) and IC_{50} values determined from *E. coli* SH399-derived fluorescence data for the full set of 9 compounds (column 2, y axis). The 3 compounds that produced outlying data are labeled in the graph. Note that neamine was excluded from the analysis due to its very weak ribosome inhibition and growth inhibition activities. Further discussion of these results is presented in the main article.

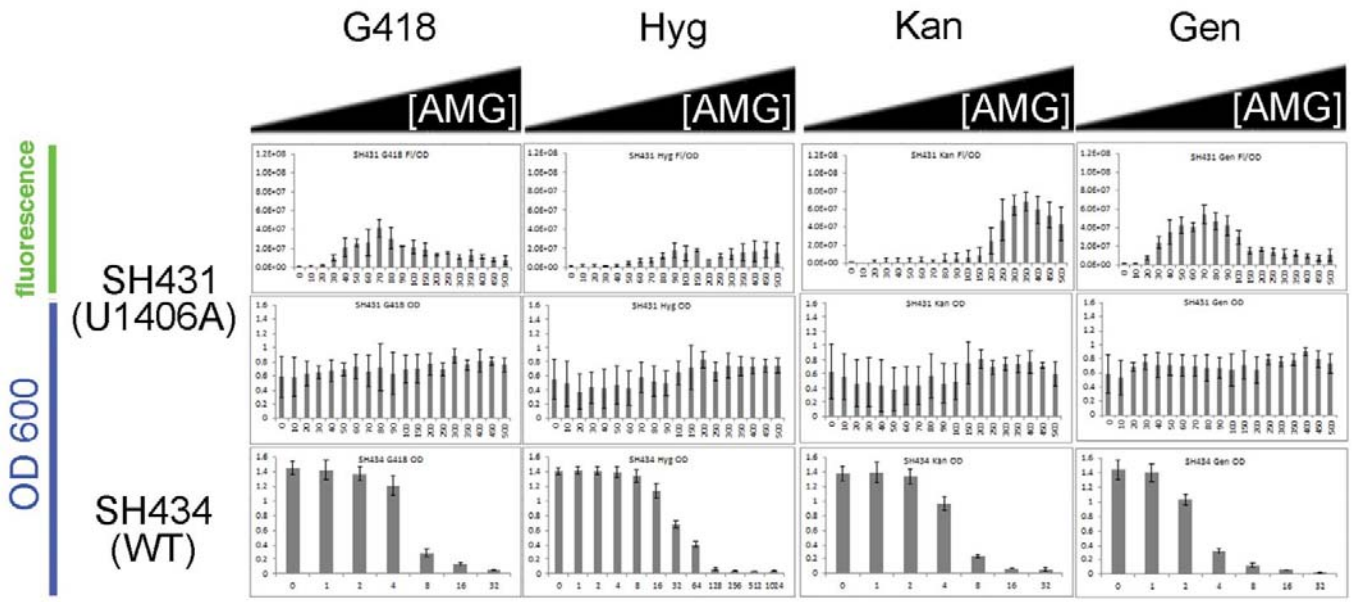

Figure S7. Fluorescence quantification (top row of graphs) and OD_{600} quantification (bottom row of graphs) of *E. coli* SH431 (pSH6-KF, pRRSH2-U1406A) cells grown in a range of concentrations (0-500 µM) of G418, hygromycin, kanamycin, and gentamicins. The scale of x and y axes is consistent for each row of bar charts. Further discussion of these results is presented in the main article.

AMG	LD_{50} (uM)	IC_{50} (uM)
Gen	2.9	32.8
G418	6.1	39.6
Hyg	31	73.3

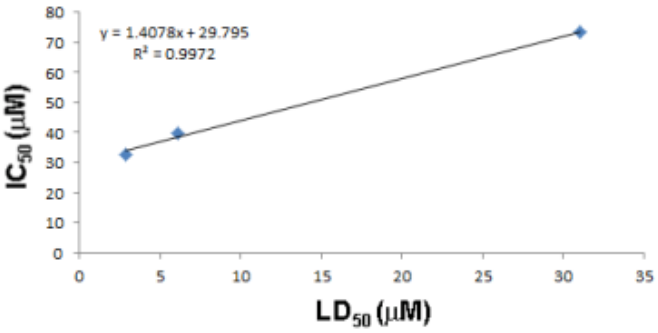

AMG	LD_{50} (uM)	IC_{50} (uM)
Gen	2.9	32.8
Kan	5.5	220.5
G418	6.1	39.6
Hyg	31	73.3

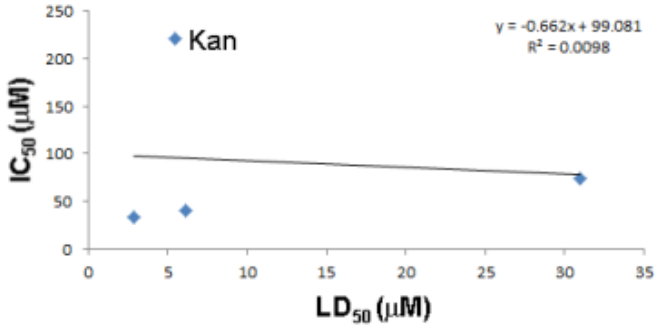

Figure S8. Analysis of the correlations between: (top table and graph) LD_{50} values determined from growth inhibition assays of *E. coli* SH434 (column 1, x axis) and IC_{50} values determined from *E. coli* SH431-derived fluorescence data for the subset of 3 compounds for which there was a statistically significant correlation (column 2, y axis); and (bottom table and graph) LD_{50} values determined from growth inhibition assays of *E. coli* SH434 (column 1, x axis) and IC_{50} values determined from *E. coli* SH431-derived fluorescence data for the full set of 4 compounds (column 2, y axis). The compound that produced outlying data is labeled in the graph. Further discussion of these results is presented in the main article.

References:

[1] J. Sambrook, D. W. Russell, *Molecular cloning: a laboratory manual 3rd edition*, Cold Spring Harbor Press, Cold Spring Harbor, NY, **2001**.

[2] D. Zaprojets, S. French, C. L. Squires, *J. Bacteriology* **2003**, *185*, 6921-6927.

[3] J. Brosius, A. Ullrich, M. A. Raker, A. Gray, T. J. Dull, R. R. Gutell, H. F. Noller, *Plasmid* **1981**, *6*, 112-118.

[4] J. Quan, J. Tian, *Nat. Protocols* **2011**, *6*, 242-251.

[5] C. E. Melançon III, P. G. Schultz, *Bioorg. Med. Chem. Lett.* **2009**, *19*, 3845-3847.

[6] C. F. Beck, R. Mutzel, J. Barbé, W. Müller, *J. Bacteriol.* **1982**, *150*, 633-642.

[7] T. S. Young, I. Ahmad, J. A. Yin, P. G. Schultz, *J. Mol. Biol.* **2010**, *395*, 361-374.

[8] V. K. Mutilak, J. C. Guimaraes, G. Cambray, C. Lam, M. J. Christoffersen, Q.-A. Mai, A. B. Tran, M. Paull, J. D. Keasling, A. P. Arkin, D. Endy, *Nat. Methods* **2013**, *10*, 354-360.

[9] V. K. Mutilak, J. C. Guimaraes, G. Cambray, Q.-A. Mai, M. J. Christoffersen, L. Martin, A. Yu, C. Lam, C. Rodriguez, G. Bennett, J. D. Keasling, D. Endy, A. P. Arkin, *Nat. Methods* **2013**, *10*, 347-353.

[10] K. Lee, C. A. Holland-Staley, P. R. Cunningham, *RNA* **1996**, *2*, 1270-1285.

[11] N. M. Abdi, K. Frederick, *RNA* **2007**, *11,* 1624-1632.

[12] S. Inouye, M. Inouye, *Nucleic Acids Res.* **1985**, *13*, 3101-3110.

[13] Y.-J. Chen, P. Liu, A. A. K. Nielsen, J. A. N. Brohpy, K. Clancy, T. Peterson, C. A. Voigt, *Nat. Methods* **2013**, *10*, 659-664.